Solvent effect and surface free energy

Investigations of solvent vapour annealed poly(isoprene-*b*-styrene) thin films and its constituents

Authors:

Christian Kjeldbjerg Kristensen
Mark Francis Brogaard Railton
Asger Lindhardt Jensen

Supervisor:

Dorthe Posselt

Roskilde University
Master Project in Physics
January 21, 2019

1 Abstract

The self-assembly process of diblock copolymers in thin films is the overall topic of this master student project in physics. When such diblock copolymers are in thermodynamic equilibrium they will form ordered structures, for instance lamellar sheets or cylinders. The self-assembly process is understood to be hindered due to the film casting method. The casting method will often disturb polymers causing them to be trapped in a metastable state. In order to direct this self-organisation an annealing process is required. One such process is subject to investigation, namely solvent vapour annealing. During annealing the polymer film will increase in thickness and the mobility of the polymer chains is increased such that the equilibrium state can be reached.

This project examines the effect the solvents toluene and heptane have on the swelling behaviour of polyisoprene, polystyrene and diblock copolymer poly(isoprene-*b*-styrene). The annealing process with both solvents was performed at room temperature while some samples were be annealed with toluene at 50°C. When annealing with toluene vapour a thickness increase around 5% was observed, both at room temperature and at 50°C. It was observed that the swelling curves for polystyrene thin films, when annealing with toluene, did not show the same stepwise increase in thickness as polyisoprene, which we ascribe to its comparatively high T_g and thereby decreased mobility. It was found that heptane was a poor choice for annealing $<50nm$ thin films of poly(isoprene-*b*-styrene) in the vapour annealing process at room temperature. In addition, this project has found no clear evidence suggesting that the cleaning techniques used for our silicon wafers had any influence on the swelling behaviour or the surface free energy of the films, which were found using contact angle measurements. Finally it was found that the polar part of the surface energies of the poly(isoprene-*b*-styrene) thin films was higher than that of its constituents while the dispersive part was closest to that of the polystyrene films. It was found that the surface energy of the diblock films were approximately equal to that of the polystyrene films, therefore we presume that the diblock films are ordered in lamellar structures, with styrene being at the air-polymer interface.

Contents

1 Abstract **1**

2 Introduction **4**
2.1 Problem formulation 4
2.2 Methodology 5

3 Theory **6**
3.1 Polymers 7
3.2 Block Copolymer Thin films 7
3.3 Characterising Polymers 9
3.3.1 Glass Transition Temperature 9
3.3.2 Solubility and Interaction Parameter 11
3.4 Solvent Vapour Annealing 12
3.5 Optical Spectroscopy 12
3.6 Surface energy 13
3.7 Contact angle 14
3.8 OWRK-method 15

4 Methods **17**
4.1 Wafer Preparation Methods 17
4.1.1 Plasma Cleaning 17
4.1.2 Piranha Cleaning 17
4.2 The Wafers 18
4.3 The Annealing Setup 20
4.4 Film thickness measurement 21
4.5 Surface free energy measurement 23
4.6 Logbook 24

5 Results and Discussion **25**
5.1 Solvent Vapour Annealing 25
5.1.1 University Wafers 26
5.1.2 The Silicon Oxide Layer, Software Tweaks and Odd Data 27
5.2 Vapour Annealing Topsil Wafers with Toluene 30

5.3 Vapour Annealing Topsil Wafers with Heptane 34
5.4 Contact angle results 37

6 Conclusion **40**

7 Perspective **42**

References **47**

A Appendix **50**
A.1 Contact Angles - Water 50
A.2 Contact Angles - Diiodomethane 51
A.3 Thickness Measurements of Oxide layer 52
A.4 Logbook explanation 53

2 Introduction

A method of generating nanostructured polymer thin film on silicon wafers is to coat them with a block copolymer solution using spin coating, and then annealing the film with solvent vapour. The final structure of the film depends on a number of factors, two of them being the structure of the wafer and how the wafer is prepared prior to coating [1].
The surface free energy of any surface, coated or not, depends directly on the binding forces of the material and will be approximated using Owens, Wendt, Rabel and Kaelble (OWRK) method, which utilises contact angle measurements between a solid surface and drops of two different types of liquid.
The polymers are applied to the wafers using spincoating with a drop of polymer solution containing each of the following; polyisoprene, polystyrene and a diblock copolymer of the two. In order to generate the nanostructured polymer thin films of the diblock copolymer we will use solvent vapour annealing. The annealing process will also be used on the polyisoprene and polystyrene samples in order to investigate and compare their swelling behaviour as well as the diblock copolymer at different temperatures. The purpose of this is to see if the different types of wafers affect the swelling process of different polymers in different temperature conditions vapour annealed with different solvents. The swelling behaviour will be monitored using optical spectroscopy at all steps. We will likewise check the surface free energy prior to and after annealing to see if annealing the thin films of diblock copolymer has a noticeable influence on the surface free energy.

2.1 Problem formulation

How does temperature and silicon wafer cleaning method influence surface free energy and swelling behaviour when vapour annealing polystyrene, polyisoprene and diblock poly(isoprene-*b*-styrene) thin films with toluene and heptane?

2.2 Methodology

In order to provide an answer to this problem, general theory about polymers is presented in section 3, such as the composition of polymers. Since solubility and the glass transition temperature of polymers are important factors when vapour annealing, theory about these are presented in 3.3. The swelling behaviour, that is dependent on the solubility parameters and glass transition temperatures, is documented using optical spectroscopy. Theory about optical spectroscopy is therefore presented in section 3.5, whereas information about the method used to measure the film thicknesses is presented in section 4.4. The validity of the absolute values of these measurements are discussed in sections 5.1 and 5.1.2. As with spectroscopy, theory about vapour annealing is presented in section 3.4 and the method used in section 4.3. Since we are investigating how cleaning methods influence swelling behaviour, the cleaning methods used are presented in the method section 4.1. Our findings on how the temperature and cleaning methods influenced the swelling behaviour when using toluene is presented in section 5.2. Due to limitations, we have only swelled with heptane at room temperature. We have also not investigated if cleaning methods influence the swelling behaviour when using heptane. How heptane influenced the swelling behaviour is discussed in section 5.3.

Theory about surface free energy is presented in section 3.6, as well as our idea about how to use surface free energy to determine the structure of the annealed block copolymer. Since determination of surface free energy requires the use of contact angles, theory about contact angles is presented in section 3.7. The model used to determine surface free energy is the OWRK-method, which is described in section 3.8. The actual method used to determine the surface free energy is presented in section 4.5.

Our findings about how temperature, cleaning and annealing influence the surface free energy is presented in 5.4. Section 7 is a combination of suggestions for further study and relevant observations not mentioned in the project itself. Since there are a lot of variables in this project, the wafers themselves and their labelling are presented in section 4.2. The usage of the experimental (digital) logbook is presented in section 4.6.

3 Theory

In this section the theoretical minimum needed to understand the results will be outlined. This project will investigate thin films made from three different kinds of polymers. The thickness of the films will be in the order of 10-100nm and will be cast on to silicon wafers employing the method of spin coating. The polymers subject to investigation during this project are the two homopolymers, polyisoprene and polystyrene, shown in figure 3.1, as well as the diblock copolymer; poly(isoprene-*b*-styrene). A collection of parameters relevant to our investigation are presented in table 1 and the meaning of these parameters will be presented in section 3.3.

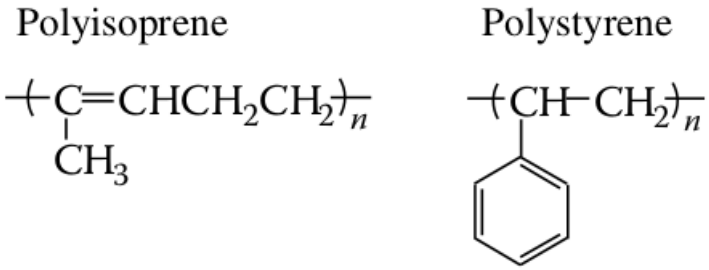

Figure 3.1: *The molecular formula for the repeat unit in polyisoprene and polystyrene, both have two bonding sites denoted with a line through a parenthesis. The n-subscript means the unit is repeated n times.*

Material	T_g [$°C$]	δ [MPa]	n	Surface free energy [mN/m]
Polystyrene	100	18.3*	1.5894	∼40
Polyisoprene	-69	16.5*	1.5191	32
Poly(styrene-isoprene)	∼	∼	∼1.5	∼
Toluene	∼	18.2*	∼	∼
Heptane	∼	15.4*	∼	∼

Table 1: *Relevant parameters for polymers and solvents used. The data marked with * is taken from [2] and the rest is looked up on* `https://polymerdatabase.com`.

3.1 Polymers

A polymer is a large molecule consisting of many repeat units, called monomers. Covalent bonds[1] link these monomers together to form complex macromolecules in many patterns [3]. A monomer is a class of small molecules which have two or more bonding sites that can be linked to other monomers (eg. see figure 3.1). One type of monomers linked together forms what is called a homopolymer, usually referred to as a polymer. Two or more varieties of monomers joined will form a copolymer.
There are different kinds of copolymers, for instance statistical and alternating copolymers that have a chain of monomers with random and periodic order respectively [3]. But the class of copolymers of interest for this investigation, namely block copolymers, is characterised by having collections of one type of monomer linked to collections of a second monomer type (ie. on the form AAA-BBB or AAA-BBB-AAA). The collections of each chemically indistinguishable group of monomers are what we refer to as blocks. Common examples of block copolymers include: diblock copolymers which are block copolymers made up of two distinct blocks, triblock copolymers composed of three distinct blocks and star triblock copolymers that are triblock copolymers where the blocks are bonded together at a central point [4].
One interesting property of block copolymers is that they will microphase separate into periodic ordered structures, determined by the interaction parameter χ between the different blocks, the degree of polymerisation N and the ratio of chain length of polymer A to polymer B. This ratio is denoted by f_A.

3.2 Block Copolymer Thin films

When forming a thin film of block copolymers chemical incompatibility between the different blocks results in mesoscale architectural compositions, where regions of chemically indistinct blocks collect when in thermal equilibrium. In the case of poly(isoprene-*b*-styrene) diblock copolymers this structure will resemble one of the compositions illustrated in figure 3.2. The exact

[1] A covalent bond is an intramolecular bond between two atoms in which an electron pair is shared between them, this creates a very strong bond.

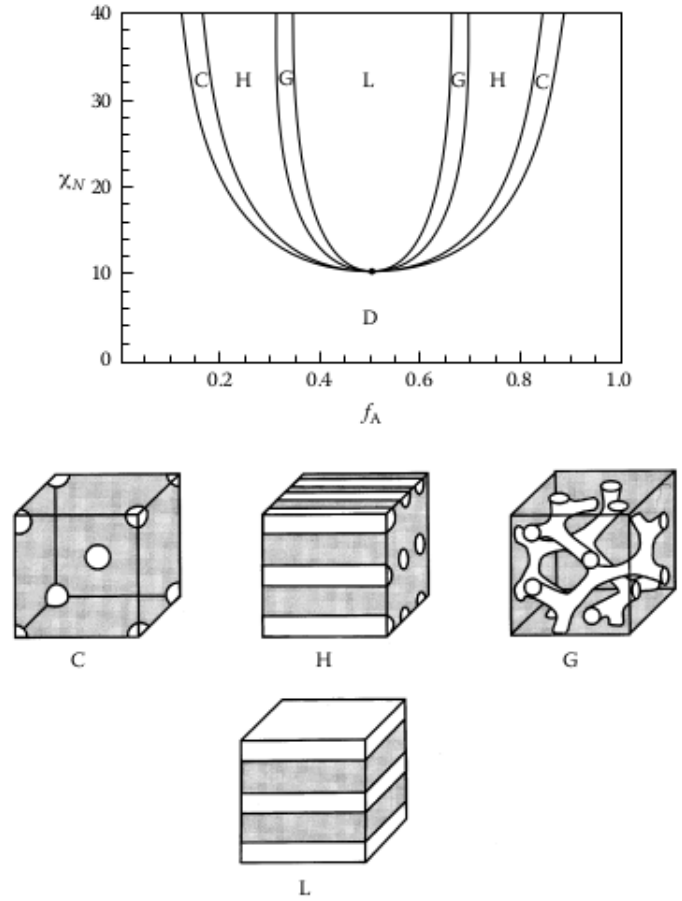

Figure 3.2: *Phase diagram for a theoretical diblock copolymer. Increasing volume fraction f_A on the first axis and the product χN, the Flory-Huggins interaction parameter for the forces between the different blocks times the degree of polymerisation N. The H-region is where cylindrical structures are formed, while the L-region is where the diblock will form lammelar structures. The figure is from [3].*

composition depends on the interfacial energy between the substrate and the possible interfaces of each composition, together with the degree of interaction between the different blocks. In the case of lammelar structures this will result in horizontal or vertical symmetry as seen of figure 3.2.
Thin films of polymers can be coated onto small surfaces in a process known as spin coating. This is the process of applying a solution containing the polymers onto the surface then spinning said surface thus coating it using

centrifugal force. The solvent used in the coating process will evaporate leaving only an even residual layer of polymer thin film. The thickness of the film is proportional to the concentration of the polymer solution and inversely proportional to the square of the angular velocity of the spincoater [5].
When the substrate has been spin coated, the polymer thin film will likely not be structured in its most ordered state, since the coating process transfers kinetic energy to the film and thereby disturbs the self-assembly process. As a result, the polymer blocks will be trapped in a metastable state. In order to bring the films into thermal equilibrium such that the block copolymers will arrange themselves in their preferred structure solvent vapour annealing can be used. The annealing process itself will be explained further in section 3.4.

3.3 Characterising Polymers

There are several parameters used in describing and differentiating between polymers, however during this project we have focused on the glass transition temperature T_g and the Hildebrand solubility parameter δ, as these parameters affect the mobility of the polymerchains in the thin films. In the following sections these parameters will be described and their implication related to the solvent vapour annealing process will be evaluated.

3.3.1 Glass Transition Temperature

All polymers are rigid and brittle solids at low enough temperature, but upon raising the temperature the polymers will acquire thermal energy which allows the polymer chains to move freely enough to flow like a viscous liquid [3].
In the solid state a polymer can be completely amorphous meaning that the polymer chains are in a random configuration with no observable order. When constant heat is applied to such a sample the temperature will (ideally) to a good approximation rise linearly, but when T_g is reached the temperature will then rise at a another rate and the polymer will soften and become rubbery [3]. A material in such a state is called a glass.
Amorphous polymers above T_g behave like rubber. Further heating of the

sample will eventually provide enough thermal energy to allow the chains to move in a viscous flow, which means the melting temperature T_m is reached. This also hints at T_g as a temperature range more than a specific temperature.
On the other hand, for an ideal crystalline polymer in the solid state, one would observe periodic ordering between the polymer chains. This will cause the sample to have a certain melting temperature T_m and no glass transition temperature [3]. This means that while heating, the temperature of the sample will rise until T_m is reached, at which point all the thermal energy goes into breaking all the bonds that hold the molecules in their lattice. When all these bonds are broken the polymer will become a viscous liquid and the temperature of the sample will rise again.
In practice most polymers will be somewhere in between the two previously mentioned cases; they will exhibit both disordering and ordering in different regions of varying sizes. Hence they will be characterised by both T_g and T_m. The polymers we are investigating in this project are polystyrene and polyisoprene with T_g at $100°C$ and -69°C respectively. At room temperature we will therefore observe polystyrene as a hard and glassy solid, and polyisoprene as a rubber-like material.

Influence of film thickness on T_g This paragraph is based on [6]. There is evidence that the glass transition temperature is affected by the thickness of the polymer thin film. The T_g of a thin polymer film on a substrate with low interaction with the polymer, has been found to lower with decreasing film thickness. It was suggested to be caused by the presence of a liquid-like layer at the polymer-air interface. But when the polymer film is cast onto a substrate that has a high interaction with the film (ie. Si-wafers), the T_g was found to increase with decreasing film thickness. In [6] results are presented that show that the T_g at the top most layer (polymer-air) is much lower than the bulk T_g, and that T_g increases with depth. At depth corresponding to the substrate-polymer layer the glass transition temperature approaches T_g in the bulk. Kim et al. (2011) provides results that show that the T_g of poly(2-vinylpyridine) and poly(methyl-methacrylate) decreases when the film thickness increases, and they refer to experiments made by others that shows

the same behaviour occurs in films made of polystyrene. At present moment the group has not had the time to further look into these experiments. Film thicknesses at $50nm$ and below is shown to have the most dramatic effect on T_g.

3.3.2 Solubility and Interaction Parameter

The Hildebrand solubility parameter of a polymer denoted δ is the parameter that tells us which solvents are most likely to dissolve the polymer. The closer the Hildebrand parameter for the polymer is to the Hildebrand parameter for the solvent, the higher the likelihood of the polymer being dissolved by the solvent.
The Hildebrand solubility parameter is defined as the square root of its cohesive energy density $e_{coh} = E_{coh}/V$ and thus $\delta = \sqrt{e_{coh}}$. The cohesive energy is the energy per molar volume associated with the net attractive forces of the chemical (polymer or solvent). Because of the relatively large molecular weight of polymers the Hildebrand solubility parameter does not change significantly at higher temperatures compared to smaller molecules [2].

Flory-Huggins Interaction Parameter To assign a measure of the interaction between the polymer chains and the solvent the Flory-Huggins interaction parameter χ has been introduced, the parameter is also used to describe the polymer-polymer interaction [7]. During the investigation for this project the group has not looked further into the details behind the derivation of this parameter, since we found it out of our scope to achieve more than a conceptual understanding of the Flory-Huggins interaction parameter.
Complete miscibility is expected if δ (and the degree of hydrogen bonding) for any given solvent and solute is similar [2].
The Hildebrand solubility parameter can be related to the enthalpic component of the Flory-Huggins interaction parameter between polymer-solvent by the following equation

$$\chi_H = \frac{V_i}{RT}(\delta_i - \delta_j)^2, \tag{3.1}$$

where index i refer to the solvent and j to the polymer and V_i is the volume of component i [2].

3.4 Solvent Vapour Annealing

As mentioned in section 3.2 block copolymers will self-assemble into ordered microdomains. After spin coating the block copolymer film has not reached its thermodynamic equilibrium state, but is trapped in a metastable state [8]. It should be noted that this metastable state is not necessarily to be understood as completely unordered. The kinetic energy from the spin coating process interrupts the self-assembling of the block copolymers, therefore the structure of the film is not ordered like in the equilibrium state. In order to let the block copolymer film microphase separate, annealing is often required. When using a normal annealing process in which the material is heated above the glass transition temperature T_g, diffusion processes eventually cause the equilibrium state to be reached. This process often is of very long duration for high molar mass systems [8]. In order to speed up the annealing time an alternative and relatively new process can be used, namely solvent vapour annealing. This process allows the annealing to take place below the T_g of the polymers in the bulk system, by introducing a solvent vapour into a chamber holding the block copolymer film. This leads to swelling of the film, effectively lowering the T_g for the system causing the film to be more fluid - allowing the block copolymers to be more mobile and diffuse into the highly ordered structure.

3.5 Optical Spectroscopy

This section is mainly based on chapter 34 in [9]. In order to measure the thickness of the thin films during annealing we will use optical spectroscopy. Optical spectroscopy works by looking at the reflectance of an incident beam of light as every material reflects light but in varying degree. The light that is not reflected at the air-film interface will propagate through the material. This will cause different intensities at different wavelengths to be transmitted back. In the end the reflected light will interfere with the incident light and cause negative interference at some wavelength and positive at others,

depending on the thickness of the film. It is the superposition of the reflected light and the transmitted light from the film that allows the film thickness to be measured.

If I_x is the intensity of the reflected light from some sample x and I_o the intensity of the emitted light from the light source, then the reflectance of x is given by $R_x = \frac{I_x}{I_o}$. Since we do not know the value of I_o one can use a reference sample in order to eliminate I_o. If the reflectance of the reference and sample is given by R_{ref} and R_{sample} respectively, then I_0 can be eliminated by

$$\frac{R_{sample}}{R_{ref}} = \frac{I_{sample}}{I_{ref}} \Leftrightarrow R_{sample} = \frac{I_{sample}}{I_{ref}} R_{ref} \tag{3.2}$$

Using refractive indices, denoted by n, it is possible to calculate the reflectance. An in-depth description of how this is done will be omitted since it is not in the scope of this project.

3.6 Surface energy

Before presenting the concept of surface free energy, we will introduce the concept of surface tension of a liquid at the vapour-liquid interface. This section is based on [10].

When averaged over time, the forces acting on a molecule inside the bulk of a liquid can be considered isotropic. But at the interface, the forces acting on a molecule from the bulk are stronger than the forces acting from the vapour, thus pulling the molecule towards the bulk. This results in a minimisation of the surface area. In order to increase the surface area, work is needed to bring the molecule from the bulk to the surface. The required (work) energy per unit surface area created is the surface free energy.

For a liquid, the surface free energy can also be thought of as a force per unit length. When the surface area of a liquid is being extended by applying a force tangentially to the surface of the liquid, molecules are being brought from the bulk onto the surface. This generates a surface tension resisting the extension. Given that γ denotes the surface tension, the force exerted by the surface tension is given by

$$F = \gamma x \quad , \quad [\gamma] = N/m \approx d/m^2 \tag{3.3}$$

whereas the change in surface free energy ΔG (work of extension) is given by

$$\Delta G = F\Delta y = \gamma x \Delta y = \gamma \Delta A \tag{3.4}$$

One of the objectives of our surface free energy measurements is to try to determine how the surface structure is and in which way the lamellar structures in the diblock copolymer thin film, is oriented. The lamellae can be oriented either horizontally or vertically, and this could be evident in the measured value of surface free energy of our poly(isoprene-*b*-styrene) thin films. If we find the surface energy of poly(isoprene-*b*-styrene) to be approximately equal to the average of the measured values of the homopolymers polystyrene and polyisoprene. We can use this as a hint that the lamellae are oriented vertically. On the other hand if we find the surface free energy to be approximately equal to the measured value for either polystyrene or polyisoprene, we take this as a hint that the lamellae is oriented horizontally with the respective homopolymer collected in the top-layer. It is also possible that the vertically aligned lamellaes can result in a more rough surface than compared to a film with horizontally aligned lamellae.

3.7 Contact angle

This section is based on [10]. A drop of liquid placed on a solid surface contains three different interfaces; the gas-liquid (L), liquid-solid (LS) and gas-solid (S) interface. Let $\Delta G_L = \gamma_L \Delta A, \quad \Delta G_{LS} = \gamma_{LS}\Delta A \quad$ and $\Delta G_S = \gamma_S \Delta A$ denote the changes in surface free energy, during a small increment of surface.

As indicated by figure 3.3, we see that the total change in surface free energy along the surface is given by

$$\Delta G^S = \Delta A \gamma_{LS} - \Delta A \gamma_S + \Delta A \gamma_L cos(\theta - \Delta\theta) \tag{3.5}$$

When the liquid drop is at equilibrium, there is no change in surface free energy, thus it must be the case that

$$lim_{\Delta A \to 0} \frac{\Delta G^S}{\Delta A} = 0 \tag{3.6}$$

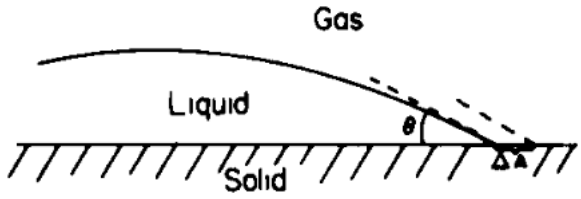

Figure 3.3: *A drop of liquid on a solid surface in contact with some gas (eg. air), and the triple point of contact between gas-liquid-solid. The angle between the tangent to liquid surface at the triple point is denoted θ and the dashed lines resembles a small increment in the surface area, ΔA. Figure is from [10].*

This gives us that

$$\gamma_{LS} - \gamma_S + \gamma_L cos(\theta) = 0 \tag{3.7}$$

which is the same equation empirically found by Young.

3.8 OWRK-method

Owens, Wendt, Rabel and Kaelble distinguished between disperse and polar interactions between molecules and proposed that they both contribute to the interfacial tension [11]. The dispersive interactions are caused by Van der Waals forces and contribute to the interfacial tension by the amount γ_x^D. The polar interactions are caused by Coulomb interactions between dipoles and contribute to the interfacial tension by the amount γ_x^P, thus giving a total interfacial tension of

$$\gamma_x = \gamma_x^D + \gamma_x^P$$

Values of γ_x^D and γ_x^P have been found experimentally for several liquids, using methods not considered in this project.
OWRK proposed that γ_{LS} is given by

$$\gamma_{LS} = \gamma_L + \gamma_S - 2\left(\sqrt{\gamma_L^D \gamma_S^D} + \sqrt{\gamma_L^P \gamma_S^P}\right) \tag{3.8}$$

Combining this with (3.7) yields

$$\frac{\gamma_L}{\sqrt{\gamma_L^D}} \frac{1 + cos\theta}{2} = \frac{\sqrt{\gamma_L^P}}{\sqrt{\gamma_L^D}} \sqrt{\gamma_S^P} + \sqrt{\gamma_S^D} \tag{3.9}$$

which is a linear equation with just two unknown parameters, $\sqrt{\gamma_S^P}$ and $\sqrt{\gamma_S^D}$. Since θ can be measured using a contact angle experiment and we know the values of γ_L, $\sqrt{\gamma_L^D}$ and $\sqrt{\gamma_L^P}$ for several liquids, we can by using two different liquids determine the values of $\sqrt{\gamma_S^P}$ and $\sqrt{\gamma_S^D}$. The surface free energy will then be given by

$$\gamma_S = \gamma_S^P + \gamma_S^D$$

.

4 Methods

4.1 Wafer Preparation Methods

The two cleaning methods applied to wafers, which were used in this project, are briefly outlined below.

4.1.1 Plasma Cleaning

Using ionised gas in a low pressure vacuum chamber the silicon wafer can be cleaned. This works by energising the gas using radio frequency power making the ions vibrate. These vibrating ions scrub the surface of the wafer removing organic contaminants. Plasma cleaning is an inexpensive and environmentally safe method to remove organic residue [12][13].
For our silicon wafers a pressure of $500mTorr$ and a processing time of 2 minutes was used in the Harrick Plasma cleaner PDC-002. The plasma used was water vapour and air. In both cases the plasma cleaner was set to its highest radio frequency power setting that uses $30W$.

4.1.2 Piranha Cleaning

Piranha solutions are usually made from a 3:1 mixture of sulfuric acid and 30% hydrogen peroxide used to dissolve organic residue. The solution is made by slowly mixing the sulfuric acid into the hydrogen peroxide while stirring due to the process being very exothermic and the mixture exceeding 100°C during preparation. The solution should be allowed to cool off before cleaning can begin. When cleaning wafers using the piranha solution the substrate is slowly submerged in the solution which is freshly made for the cleaning process since storage of the mixture is extremely dangerous. Explosions have been known to occur when the solution is improperly prepared or comes in contact with solvents such as acetone. The solution should never be kept in a sealed container due to its propensity to explode [14].

4.2 The Wafers

For our experiments we will be using the silicon wafers presented in table 2. All wafers excluding the ones denoted IS1 through IS8 and the associated uncoated wafer were procured from Topsil GlobalWafers A/S while the aforementioned exclusions were obtained from UniversityWafer inc. All coated University Wafers have been spincoated with the styrene-isoprene block co-polymer. The naming convention for the Topsil wafers used throughout this report is as follows: [*polymer*][*cleaning method*][*number*]. The polymer entries are "C" for the block co-polymer, "I" and "S" for isoprene and styrene respectively while "B" denotes the blank uncoated wafers. The cleaning method entries "PA", "PW", "Pi" and "To" refer to plasma cleaned with air, plasma cleaned with water, cleaned using a piranha solution and wafers uncleaned after obtainment respectively. It should be noted that we as of writing are unaware of the exact treatment applied to the wafers by Topsil prior to their acquirement. Lastly coated Topsil wafers with number entries 1 to 3 are spincoated at $6krpm$ in solutions of $2wt\%$ (weight by percentage) while number entries 4 to 6 denote wafers spincoated at $3krpm$ in solutions of $3wt\%$. $krpm$ and $wt\%$ for University wafers can be looked up in table 2. All wafers mentioned come with a native silicon oxide layer. The oxide layer thickness is expected never to be much more than $2nm$ due to the self-limiting nature its formation.[15] A single measurement has been conducted for us using ellipsometry, found in table 3, which tells us that this layer is $\sim 1.5nm$.

Sample ID	Material	krpm	wt%	Cleaning method	Suplier
CPA1	Isoprene-Styrene	6	2	Plasma Air	Topsil
CPA3	Isoprene-Styrene	6	2	Plasma Air	Topsil
BPA1	Blank	-	-	Plasma Air	Topsil
IPW1	Isoprene	6	2	Plasma H2O	Topsil
IPW4	Isoprene	3	3	Plasma H2O	Topsil
IPW5	Isoprene	3	3	Plasma H2O	Topsil
SPW1	Styrene	6	2	Plasma H2O	Topsil
SPW4	Styrene	3	3	Plasma H2O	Topsil
CPW1	Isoprene-Styrene	6	2	Plasma H2O	Topsil
CPW3	Isoprene-Styrene	6	2	Plasma H2O	Topsil
CPW4	Isoprene-Styrene	3	3	Plasma H2O	Topsil
CPW5	Isoprene-Styrene	3	3	Plasma H2O	Topsil
CPW6	Isoprene-Styrene	3	3	Plasma H2O	Topsil
BPW1	Blank	-	-	Plasma H2O	Topsil
CPi1	Isoprene-Styrene	6	2	Piranha	Topsil
CPi2	Isoprene-Styrene	6	2	Piranha	Topsil
CPi4	Isoprene-Styrene	3	3	Piranha	Topsil
CPi5	Isoprene-Styrene	3	3	Piranha	Topsil
BPi1	Blank	-	-	Piranha	Topsil
ITo1	Isoprene	6	2	-	Topsil
CTo1	Isoprene-Styrene	6	2	-	Topsil
CTo4	Isoprene-Styrene	3	3	-	Topsil
CTo5	Isoprene-Styrene	3	3	-	Topsil
BTo1	Blank	-	-	-	Topsil
IS1	Isoprene-Styrene	1	2	-	UniversityWafer
IS2	Isoprene-Styrene	1	2	-	UniversityWafer
IS3	Isoprene-Styrene	1	5	-	UniversityWafer
IS4	Isoprene-Styrene	1	5	-	UniversityWafer
IS5	Isoprene-Styrene	2	2	-	UniversityWafer
IS6	Isoprene-Styrene	2	2	-	UniversityWafer
IS7	Isoprene-Styrene	2	5	-	UniversityWafer
IS8	Isoprene-Styrene	2	5	-	UniversityWafer
BIS1	Blank	-	-	-	UniversityWafer

Table 2: *Silicon wafers and their specifications.*

4.3 The Annealing Setup

The experimental setup consists of a sealed vapour chamber (see figure 4.1) into which nitrogen gas is pumped together with the solvent vapour. Onto the chamber a thermostat is attached allowing the temperature to be controlled during the solvent vapour annealing. The sample is then placed inside the chamber (roughly in the middle) and through the lid an optical fiber is connected such that the thickness of the film can be monitored via optical spectroscopy.

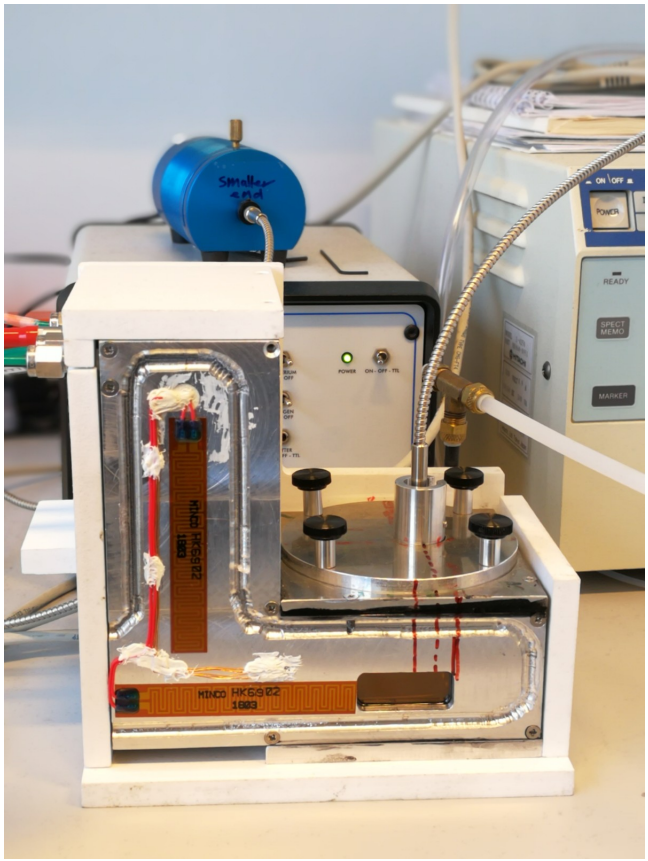

Figure 4.1: *A photograph taken of the sovlent vapour annealing chamber used during the experiments.*

The flow controllers controlling the flow of nitrogen gas and solvent vapour are provided by Bronkhorst High-Tech BV are programmed as follows:

The flow controller connected directly to the chamber is set to $400 sccm$

The flow controller connected to the bubbler containing the solvent is set to $200sccm$

The first flow controller is set to 100% until it is determined that the thickness of the thin film measured through spectroscopy is constant.

The flow controller connected directly to the chamber is then stepwise at $600s$ intervals decreased by 12.5% while the flow of the controller connected to the bubbler is stepwise increased in increments of 25% until the flow of the controller connected to the bubbler reaches 100%.

After $1200s$ the flow controller connected directly to the chamber is then stepwise at $600s$ intervals increased by 12.5% while the flow of the controller connected to the bubbler is stepwise decreased in increments of 25% until the flow of the controller connected to the bubbler reaches 0%.

After $600s$ the script terminates concluding the experiment.

4.4 Film thickness measurement

In this project the thickness of the thin film samples will be measured by using optical spectroscopy. Specifically we will be using a spectrometer from Ocean Optics Inc.
An optical fiber cable, which cross section is illustrated in figure 4.2, is attached to a halogen lamp outputting light into the chamber in figure 4.1, whereas the output is reflected back by the wafer into the cable input that is attached to a spectrometer. The spectrometer is then attached to a computer running the Ocean Optics software NanoCalc.
Not knowing how NanoCalc does its measurements, we assume that the light intensity is measured for each integer nm wavelength. In order to eliminate interference from the optical fiber itself and background light, we have put a piece of black cloth in the chamber, put the lid on, and made a light intensity measurement, called a "dark", using NanoCalc. For each wavelength, this dark intensity, I_{dark}, is then subtracted from the intensity of I_{sample} and I_{ref}

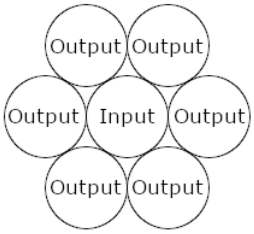

Figure 4.2: *The construction of the optic fiber cable. The halogen lamp outputs light at the six surrounding fibres, and the reflected light is sent to the spectrometer through the centre fiber.*

in equation (3.2), that is[2]

$$R_{sample} = \frac{I_{sample} - I_{dark}}{I_{ref} - I_{dark}} R_{ref} \tag{4.1}$$

where NanoCalc uses the reflectance of the substrate instead of the reference. In the NanoCalc software a "layer-structure" must be specified before a measurement can be completed, here the different layers found in the sample of investigation can be added. During this project work the following layers has been specified: 0) substrate-layer, 1) oxide-layer and 2) film-layer. Each individual layer provides a refractive index n for the chosen material. It is also possible to put limiting values on the range of search for thickness. NanoCalc uses the reflectivity of the sample to compare with a number of simulated curves, that have been generated by the refractive indices of the oxide and polymer layers, as well as estimations about the thickness of the layers. The final thickness is given by the result with the best fit between measured and simulated curve. That fitness "is the sum of the mean square deviations between measured and simulated curve (normalised to the range of extraction)" [16]. For reasons discussed in section 5.1.2, the fitness has not been taken into account and is therefore omitted from the results.

Since we are working with Si wafers with FCC(1,1,1) structure, we have used "Si(111)" for reference and layer 0. We have been using the same reference file for all of the measurements presented in section 5, except for the

[2]It should be noted, that NanoCalc stores the term $I_{ref} - I_{dark}$ as the Reference intensity

measurements done on the university wafers. As for layer 1, we have been using SiOx with an estimated guess of thickness from 0 to 50nm for the majority of our experiments[3]. Since the refractive index of the different kinds of polymer varies, we have for layer 2 been using n1_5, n1_6 and n1_55 for polyisoprene, polystyrene and poly(isoprene-*b*-styrene) respectively. The range of extraction is set to 400-1041 internally by the NanoCalc software and has not been set by the group.
Due to reasons that will be discussed in section 5.1.2, we have converted our data to be using "SiO2_(therm)" instead of "SiOx".

4.5 Surface free energy measurement

Following the recommendations from KRÜSS, we have decided to use diiodomethane and water as our two test liquids for surface free energy determination. The surface free energy of diiodomethane has no polar component due to its is highly symmetrical molecular structure [17][18]. This reduces 3.9 to

$$\gamma_L \frac{1 + cos\theta}{4} = \gamma_S^D \tag{4.2}$$

meaning that the dispersive part of the solid can be determined with only one contact angle measurement. According to KRÜSS diiodomethane has also been chosen due to its high surface energy at 50.8mN/m. Water has been chosen because of its high polarity. The polar γ_L^P and dispersive γ_L^D components of the surface free energy of water used in the software "ADVANCE" by KRÜSS is given by 51mN/m and 21.8mN/m respectively. Even though KRÜSS advises to use tap water, we have used deionized water, which might affect our final result due to impurities from the air affecting the water. Since there is a difference in surface energy between our substrate and polymer, the surface contact area increases over time due to the polymer getting dissolved in the liquids. This means that ΔA never goes to zero in equation 3.5. We have chosen to ignore this fact while doing contact angle measurements and will still be using Young's equation. We have chosen to calculate the surface free energy from the average of snapshots of the liquid drops after 0.5s, 1s

[3]It can be seen in the logbook which experiments we have been using SiOx and what out thickness estimates have been

and $1.5s$.

4.6 Logbook

A digital logbook was created on the sixth of December 2018. All the meaningful entries before that date was imported from our paper logbook. We also added a "purpose for experiment" to each entry. These purposes had not been logged in our original logbook, but has been created from memory. From then on, purposes have always been added before the entry takes place. Also, purposes have not been changed after they have been added, except when we decided to use ID numbers instead of line numbers for referencing to entries in the logbook. The comments have been added either before, during and/or after the entry have taken place. An explanation of each of the column entries can be found in appendix A.4. It should be noted that we have not updated the logbook after changing from SiOx to SiO2_(therm).

5 Results and Discussion

In the following sections results from the thickness measurements during solvent vapour annealing (sections 5.1, 5.2 and 5.3), contact angle measurements (section 5.4), as well as the challenges faced along the way will be presented and discussed.

5.1 Solvent Vapour Annealing

This first section will be focusing on the results obtained through the annealing of our thin films. It should be understood that the relative swelling of our thin films during annealing has proven to be far lower than what has been observed by Dorthe Posselt et al. in [19]. Therefore we can not confidently say if the individual thickness measurements calculated by the NanoCalc software really reflects the real thickness of the film and that the relative thickness changes are correct. With that in mind we will still be able to compare the swelling curves made during this project. Hence the focus has instead been to observe the behaviour of the thin films as they are annealed, since polymer mobility at different temperatures and concentrations of solvent vapour can be related to T_g and δ of the polymers in question. For all the swelling curves the relative thickness increase has been calculated as

$$\frac{d_{max} - d_{start}}{d_{start}} 100\%$$

In order to relate our results to more accurate thin film thickness estimates, the group acquired ellipsometry measurements for a number of the samples, but did not do the measurements themselves. The relevant results from this analysis can be found in table 3. It should be noted that we do not know exactly which samples were used for the individual ellipsometry measurements aside from how they were treated and coated given that 3 samples were created with each polymer specification for each cleaning method.

units in [nm]	CPA 2%	IPA 2%	SPA 2%	CPW 2%	IPW 2%
Topmost Layer	40.67	57.31	52.28	42.31	64.40
Certainty	±0.133	±0.21	±0.015	±0.129	±0.024

units in [nm]	SPW 2%	CPW 3%	SPW 3%	IPW 3%	BPW
Topmost Layer	59.92	100.24	103.665	108.31	1.63
Certainty	±0.019	±0.017	±0.019	±0.020	±0.003

Table 3: *Ellipsometry data. Here named by the percent by weight concentration, used during spincoating, rather than numerically. It should be noted that the topmost layer for the BPW sample is silicon oxide.*

5.1.1 University Wafers

The samples, which were prepared on substrate from University Wafers, were originally given to us mainly to practice the solvent vapour annealing process. As a demonstration of the spectroscopy setups ability to measure thicknesses of polymer thin films, table 4 is provided. Keeping in mind that the resulting film thickness of a spincoated polymer thin film is directly and inversely proportional to polymer dilution and spincoating speed respectively, the measured thicknesses seen in table 4 agree with their relative specifications. That is to say that the wafers with the thinnest films are IS3 and IS4 having been cast with the highest spincoating speed in combination with the lowest dilution; while the thickest measured are IS5 and IS6 having been cast at the lowest speed and with twice the concentration.

Sample ID	IS1	IS2	IS3	IS4	IS5	IS6	IS7	IS8
Polymer layer (nm)	39.3	38.2	30.0	32.1	71.4	68.7	51.4	54.4
Oxide Layer (nm)	0.0	0.0	0.0	0.0	0.2	0.0	0.0	0.0
Fitness	0.089	0.092	0.078	0.078	0.062	0.078	0.12	0.25
Dilution wt%	1	1	1	1	2	2	2	2
Spincoat vel. (krpm)	2	2	5	5	2	2	5	5

Table 4: *Initial spectroscopy measurements of University wafer thicknesses.*

Initial thickness measurements during annealing can be seen on figure 5.1. It is clear that poly(isoprene-*b*-styrene), at room temperature (SI1 and SI7), swells according to the stepwise increase in solvent vapour inside the chamber as expected. We observe a rise in thickness from $41.1nm$ to $47.8nm$ for SI1 and from $35.1nm$ to $45.2nm$ for SI7, so a rise of 16.3% and 28.8% respectively. The poly(styrene-isoprene) sample annealed at temperature $T = 50°C$, swells as expected in the beginning, from $35.8nm$ to $42.8nm$ (19.6%), but when we start decreasing the solvent vapour (around t=2600s) we do not observe a stepwise decrease in thickness. This is most certainly because of an error, such as the lid not being closed correctly, vapour chamber not being properly insulated leading to condensation caused by temperature differences or the like. It was these initial measurement that led to the investigation of polymer thin films consisting of homopolymers of polyisoprene and polystyrene in order to compare them to the block copolymer of poly(isoprene-*b*-styrene). It should be noted that out of the results of the 3 experiments shown only the annealing of SI7 was done according to the procedure outlined in section 4.3

5.1.2 The Silicon Oxide Layer, Software Tweaks and Odd Data

As can be seen in the logbook NanoCalc had initially been set up so that the silicon oxide layer on the substrate had a reflectance value of 2.6 which in the NanoCalc library was labeled "SiOx". We got a good fitness when using a SiOx estimate between 0 and $50nm$ and bad fitness when it was put between 0 and $10nm$. When fixing it between 0 and $10nm$, we saw less swelling compared to when fixed between 0 and $50nm$. It was then concluded that the results was better when estimating the oxide layer "SiOx" from 0 to $50nm$. It was therefore decided to go continue with the estimate between 0 and $50nm$, even though the thickness measurement of the oxide layer also showed signs of swelling.

Figures 5.2a and 5.2b show the polymer and SiOx layer thicknesses respectively during annealing calculated using SiOx as the silicon oxide layer. From

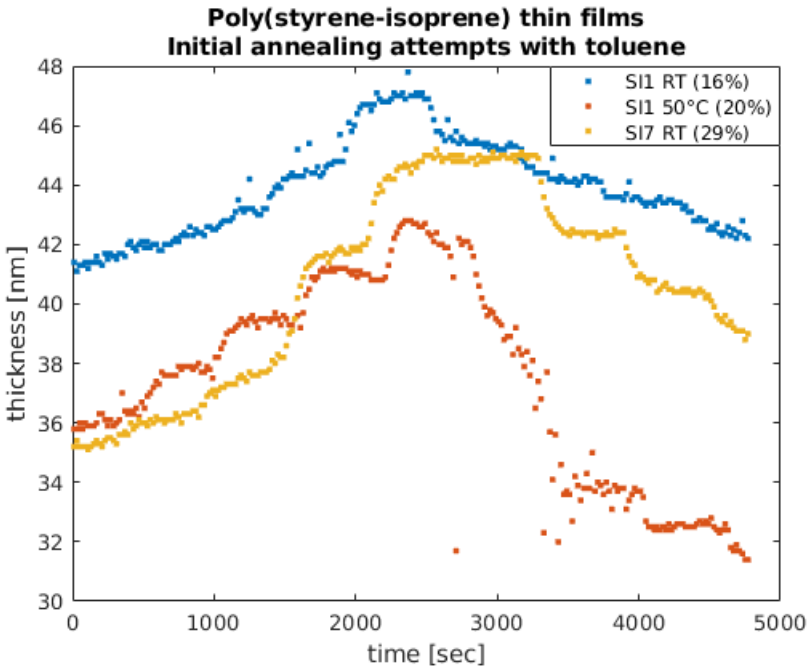

Figure 5.1: *Initial attempts at annealing. Samples of poly(isoprene-b-styrene) prepared on University Wafers, swelled at room temperature and at $T = 50°C$.*

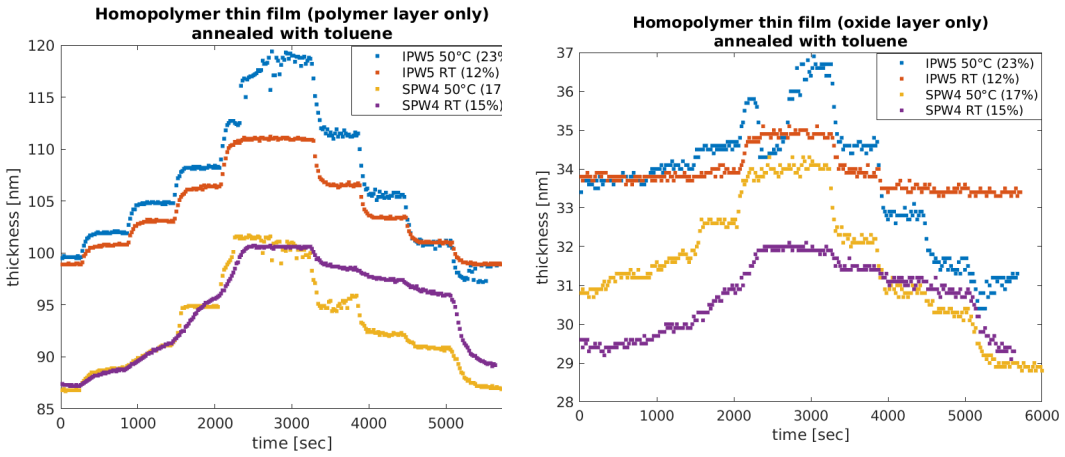

(a) *Polymer layers* **(b)** *Oxide layers*

Figure 5.2: *Thin film measurements of polystyrene and polyisoprene annealed with toluene at room temperature and 50°C. A refractive index of 2.6 has been used for the silicon oxide layer for these measurements.*

	SPW4	IPW5
SiOx layer thickness	29.6 nm	33.8 nm
Polymer layer thickness using SiOx	87.4 nm	98.9 nm
SiO2_(therm) layer thickness	1.6 nm	1.5 nm
Polymer layer thickness using SiO2_(therm)	93.7 nm	100.1 nm

Table 5: *Comparison between spectroscopy measurements when using SiOx and SiO2_(therm).*

these graphs it would seem that the oxide layers on our plasma cleaned wafers are not only much thicker than expected (here between $\sim 29nm$ and $\sim 34nm$) but also exhibit the same relative swelling as the polymer on top of it.
Though undocumented, it was later noticed that no matter what was put in the chamber it was really hard to get a bad fit when using an SiOx estimate between 0 and $50nm$. We therefore started to experiment with changing the SiOx to other types of oxides because of the better fitness. For all the "SiO2" library layer files inside the NanoCalc software library, we got oxide layer thicknesses in the same magnitude as the native oxide layer. These oxide layer thickness measurements matched the ellipsometry data better (compare table 3 and 5) and did not change as much as can be seen on figure 5.2b. The film thicknesses also matched the ellipsometry data better and the fitness also behaved more realistically (undocumented). We also noticed that the refractive index of SiOx on NanoCalc is set to 2.6, which is much higher than most silicon oxides. Normal silicon oxides have a refractive index between 1.4 and 1.9 [20]. All these findings suggest that there must be something wrong with using SiOx. Since we do not have any knowledge about the different types of SiO2 library files, we opted to use SiO2_(therm) as it had a refractive index within the range between 1.4 and 1.9 and did not take any additional parameters. A graph showing these measured oxide layers during annealing can be found in appendix A.1.
By the time the change to SiO2_(therm) was made the amount of datapoints ammassed throughout the annealings was in the thousands so to reanalyse these datapoints manually with a different n value would be unrealistic given the time consuming nature of this process and the limited time left to finish

the work.
In order to reanalyse the spectrometer data the NanoCalc analysis software and a macro recording tool[21] were installed on six computers. The keystrokes and mouse movements, needed to reanalyse the data with a different silicon oxide layer, were recorded and the data was reanalysed this way. For the datapoints recorded during the annealing of the homo polymers referred to in figures 5.2a and 5.2b, the oxide layers determined by the reanalysed data shows that the oxide layers are between $1.5nm$ and $1.9nm$ thick which is consistent with the native silicon oxide layer thickness discussed in section 4.2 as well as the ellipsometry data from table 3. The reanalysed thickness data for the polymer layers that these datapoints refer to will be coming up in section 5.2, figure 5.3.
It should be noted that the second half of the datapoints from swelling IPW5 at 50°C, seen in figure 5.2a seem to diverge from the shape of the datapoints we see when annealing IPW5 at room temperature. We have as of yet not fully identified why this happens but we also see these "jumps" when annealing diblock thin films at 50°C (see figure 5.5). These "jumps" however have only been observed when annealing at 50°C. It could possibly be caused by condensation of the solvent vapour or by the way NanoCalc calculates the thickness of the thin film. The vapour annealing of IPW5 at 50°C has been done a second time where this the "jump" did not occur which can be seen on figure 5.3. Because of this we do not find it plausible this could have been caused by an attribute of the thin film.

5.2 Vapour Annealing Topsil Wafers with Toluene

In this and the following section the thickness measurements of the polymer films prepared on Topsil wafers will be presented. The first experiments were done on films cast from polystyrene (SPW4) and polyisoprene (IPW5) which were annealed with toluene at room temperature and at 50°C. These thickness measurements can be seen in figure 5.3. We see that polystyrene (SPW4) when annealed at room temperature starts out at a thickness of $93.7nm$ and swells to a maximum thickness of $99.7nm$ which corresponds to a 6.4% increase, while at 50°C the film thickness is $92.5nm$ in the beginning

and swells to $97nm$ thus swelling just 4.9%. The thickness measurements of polyisoprene when solvent vapour annealed at room temperature and $T = 50°C$ look very similar: we observe in the beginning a thickness of $100nm$ and $99.4nm$ respectively, with a maximum of $104.1nm$ and $102.6nm$. This corresponds to a thickness increase of 4.1% and 3.2% when annealed at room temperature and at 50°C respectively. Both of these findings suggests that raising the temperature inside the annealing chamber in fact decreases the swelling behaviour.

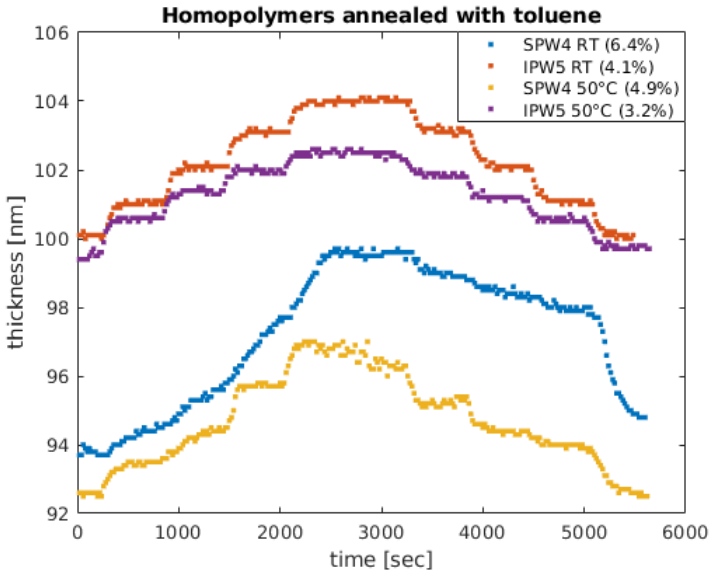

Figure 5.3: *Thin film measurements of polyisoprene and polystyrene annealed with toluene at room temperature and 50°C*

What is of most significance is the differences in the rate at which the two polymers react to the toluene. From the graph it can be seen that while the polyisoprene film thicknesses reach a plateau with each stepwise increase in solvent vapour concentration, the polystyrene film does not have enough time to plateau within the $600s$ intervals before the next step. These results suggest that the mobility of the polystyrene is low at this temperature. This is further supported by the way the polystyrene thin film annealed at 50°C seems to plateau when in the high solvent vapour density region of the graph. Though table 1 tells us that toluene should be selective for polystyrene and less so for polyisoprene, it also notes that the glass transition temperature T_g

for polystyrene is higher than the temperature at which it has been annealed and therefore the polymer is most likely a glassy solid at this point. Meanwhile polyisoprene should at these temperatures be in the rubbery phase as mentioned in section 3.3.1. This difference in mobility is likely the cause of the observed phenomenon.
The differences in polymer behaviour during swelling reflected in the results of annealing polystyrene at the two different temperature levels may be related to Akiko Yoshioka's and Kohji Tashiro's findings from [22] which show that solvents can lower the T_g of polymers. Though it is not completely clear from figure 5.3, it would seem as though a change in the behaviour of the polystyrene thin film occur when annealed at 50°C between the $1500s$ and the $4000s$ marks. It is however speculative as to whether a phase transition occurs under these circumstances without further experimentation.
In figure 5.4 the film thickness measurements of diblock poly(isoprene-*b*-styrene) annealed with toluene vapour at room temperature are presented. The three samples are identical with regards to polymer composition, but are cast on wafers prepared with different cleaning methods. Both CTo4 and CPi4 start at approximately the same thickness at $91.2nm$ and $91.1nm$ and swell to a maximum of $96.2nm$ and $96.0nm$ corresponding to a increase of 5.5% and 5.4% while CPW4 swells from $93.6nm$ to $98nm$ increasing by 4.7%. It appears the surface preparation methods used do not influence the degree to which the poly(isoprene-*b*-styrene) film swells during vapour annealing with toluene. Nevertheless this does not exclude the possibility of differences on the molecular level with respect to the ordering of the films. This will however be elucidated by contact angle measurements.

The thin film measurements of poly(isoprene-*b*-styrene) annealed with toluene at 50°C can be seen in figure 5.5. Here we observe that samples CTo5, CPi5 and CPW5 have thicknesses $91.1nm$, $91.2nm$ and $92.5nm$ in the beginning and swells a maximum thickness of $95.9nm$, $96.1nm$ and $96.9nm$ which corresponds to an increase of 5.3%, 5.4% and 4.8% respectively. When taking the propensity for errors of the measurement apparatus into account, these differences are not large enough to be considered significant. In other words, no notable difference between samples annealed with toluene at room tem-

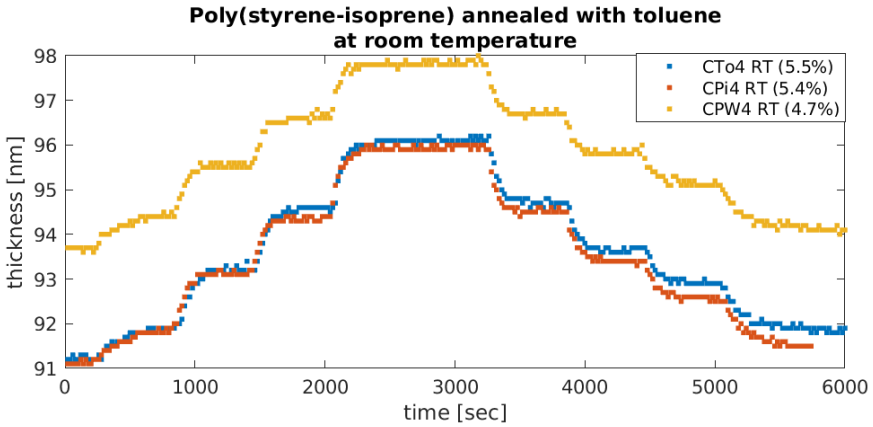

Figure 5.4: *Thin film measurements of poly(isoprene-b-styrene) annealed with toluene at room temperature.*

perature and 50°C has been established.

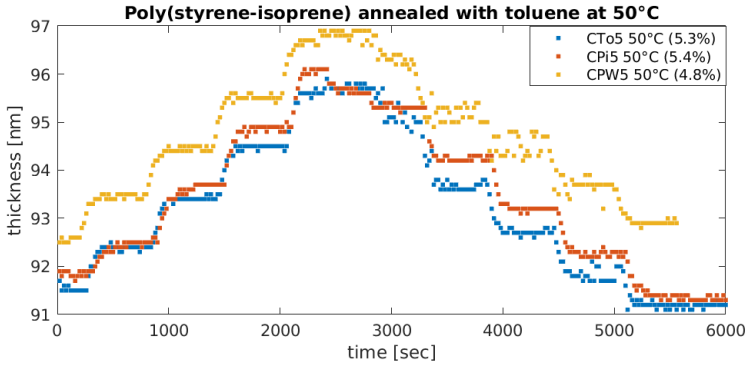

Figure 5.5: *Thin film measurements of poly(isoprene-b-styrene) annealed with toluene at* $T = 50°C$.

Attempts at annealing a thinner diblock film of poly(isoprene-*b*-styrene) than those presented until now have been made and the thickness measurements can be seen on figure 5.6. These films have a thickness of $42nm$ according to elipsometry data (see table 3), but here our measurements gives a thickness in the range of 84-87.5nm. We observe for CTo1 and CPW1 a percentwise swelling of 0.83%, while a swelling of 0.46% is calculated for CPi1. When observing the swelling curve for CPi1 it is evident that no apparent swelling has occurred. These findings seem to confirm that that T_g increases with decreasing film thickness as mentioned in section 3.3.1. Kim et al. shows in

[6] that the most dramatic effect on T_g is found in film with thickness around $50nm$ and below. Therefore, since the three diblock CTo1, CPi1 and CPW1 have thicknesses approximately in this range, the low swelling rate can be explained by the lack of mobility in the polymer film caused by an increase in T_g.

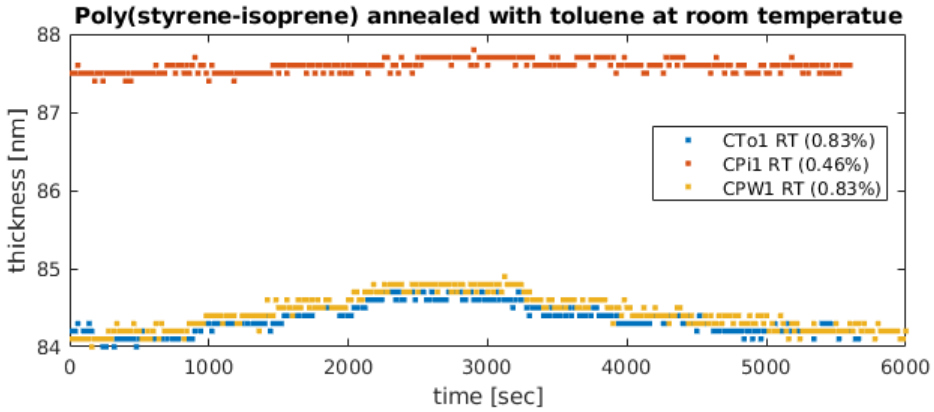

Figure 5.6: *Thin film measurements of poly(styrene-isoprene) annealed with toluene at room temperature.*

5.3 Vapour Annealing Topsil Wafers with Heptane

To observe the behaviour of the film thickness when the solvent used is selective to polyisoprene rather than polystyrene (see table 1 for confirmation), six samples were annealed with a solvent vapour of heptane. The hypothesis is that the polyisoprene will exhibit higher susceptibility to heptane than when annealed with toluene, while the polystyrene should be unaffected due to its illsuited solubility parameter on top of its high T_g. Figures 5.7 and 5.8 show the measurement results from these experiments.

From figure 5.7 it can be confirmed that heptane does indeed dissolve polyisoprene, though less than expected, but does not seem to have any noticeable effect on the polystyrene thin film. We observe a swelling of 2.9% for IPW5 and 1.1% for SPW5. This should be unsurprising when taking the results from the experiments with toluene vapour into account. It would be fair to conclude that the difference in T_g between the two homopolymers is what makes this figure so different from figure 5.3.

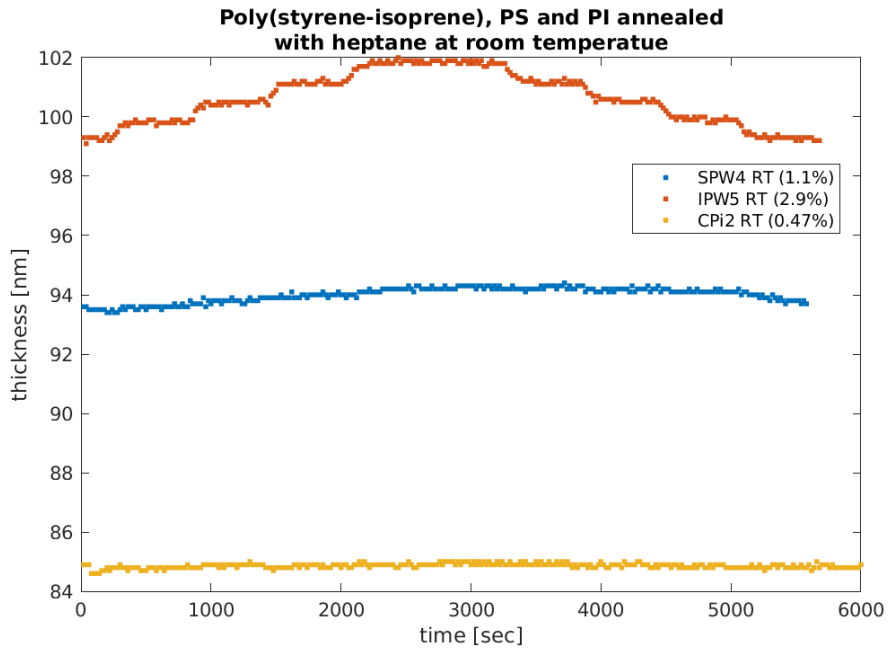

Figure 5.7: *Thin film measurements of poly(styrene-b-isoprene), polystyrene and polyisoprene annealed with heptane at room temperature*

Additionally, the diblock thin film appears to behave similarly to the polystyrene film with a swelling of just 0.47% and because of these results three additional annealing experiments were conducted with thin films of similar thicknesses as shown in figure 5.8 to see if the results will agree. As can be seen on this figure we notice a swelling of 2.2% for polyisoprene (IPW1) and 0.57% for polystyrene (SPW1), while only a thickness increase of 0.46% for the diblock film (CTo2), so the percentwise increase in thickness for this experiment corresponds to the former experiment with heptane annealing.
The explanation as to why the diblock tends to behave like polystyrene when annealing with heptane vapour and like polyisoprene when annealing with toluene could stem from the structure of the poly(styrene-b-isoprene) film. If the film has a vertically oriented lamellar structure with the polystyrene being on the topmost layer, the polystyrene could work as a protective layer preventing the heptane from penetrating the film preventing any swelling from occurring. This hypothesis will be tested using contact angle measurements. This phenomenon could also be related to the T_g dependence on the

film thickness as described in section 3.3.1. From table 3 it can be seen that the wafers in question have thicknesses of less than $50nm$ which is where the T_g for polymers tend to rise drastically. This does however not seem to be the case since figure 5.1 clearly shows that the copolymer thin films on the University Wafers exhibit swelling behaviour when annealed with toluene. Lastly, the results could be affected by measurement errors stemming from our practice of using an old reference file for new measurements.

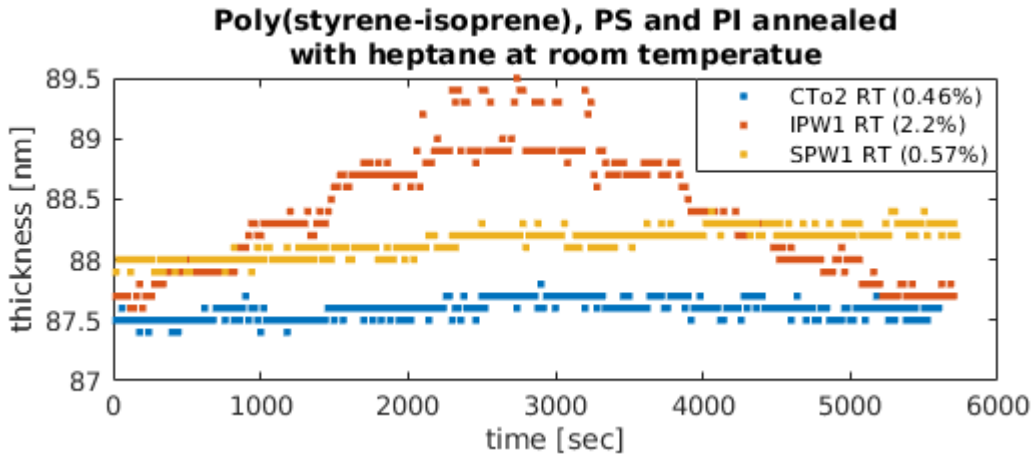

Figure 5.8: *Thin film measurements of poly(isoprene-b-styrene), polyisoprene and polystyrene annealed with heptane at room temperature.*

5.4 Contact angle results

The surface free energies from the contact angle measurements found in table 6 have been carried out in order to get the most diverse sampling group possible. This is done to test as many different parameters as possible without sacrificing too many of the samples in the process. Two of each homopolymer thin film samples of different thicknesses (IPW1, IPW4, SPW1 and SPW4) have been tested to use as reference for the block copolymers and to see if film thickness has a noticeable effect on these homopolymers. CPi2 and CTo2 have been chosen as they have been annealed with heptane. CPW6 and CPW3 have been chosen since they have not been annealed and are of different thicknesses. CPW4 and CPW5 has been chosen to see if annealing temperature influences surface free energy. CPW1, CTo1 and CPi1 have been selected to represent the different cleaning methods and to investigate if this has a noticeable effect on the surface free energy of the thin film. Lastly, the four blank wafers BTo, BPA, BPi and BPW have been chosen to test the various wafers themselves. The mean values for the contact angles measured with water and diiodomethane can be found in appendix A.1 and A.2 respectively.

The surface free energy of 4 homopolymer thin films IPW1, IPW4, SPW1 and SPW4 was measured to $38.87 mN/m$, $40.52 mN/m$, $45.67 mN/m$ and $46.50 mN/m$ respectively. Although the thinner films were measured to have a lower surface energy than their thicker counterpart, these were measured to be well within their respective uncertainty ranges. It must thus be concluded, that our findings do not show, that the thickness of the homopolymer films have any significant effect on their surface energy for the thickness ranges measured. It should also be noted that it would make little intuitive sense for the thinner films to have lower surface free energy, given the much higher surface energy of the substrate.

All surface free energy results for the block copolymer thin films measured can reach slightly above $45 mN/m$ within their respective uncertainty ranges; their respective dispersive and polar parts do not diverge noticeably outside their uncertainty ranges. Therefore we conclude, that our findings do not

show, that the surface energy observed on our block copolymer thin films revealed any noticeable difference between the different cleaning methods or solvent vapour used on our wafers.

Taking the averages of the polymers an estimated value for their respective surface free energies can be approximated and compared. These averages are $39.7mN/m$ for polyisoprene, and $46.1mN/m$ for polystyrene, their overall average $42.9mN/m$ and the poly(isoprene-*b*-styrene) $45.1mN/m$. These numbers suggest that the block copolymer thin film at its surface, with regards to its surface free energy, resemble polystyrene thin film more than the calculated average of $42.9mN/m$ between the two homopolymers. This is further evidence in favour of a lamellar structure inside the block copolymer thin film with the styrene blocks located the film-air interface.
This reasoning however is only partially supported when looking at the averages of the dispersive and polar parts separately. The overall dispersive part average of the homopolymers is $42.3mN/m$ while the average for the diblock thin films is at $43.3mN/m$ and the polystyrene films $45.0mN/m$. Meanwhile, the averages for the polar parts of polyisoprene, polystyrene and the diblock thin films are $0.045mN/m$, $1.14mN/m$, and $1.9mN/m$ respectively. This tells us that the diblock films have a higher polar part than what its constituents would suggest.

Measurement name	Surface free energy [mN/m]	Disperse [mN/m]	Polar [mN/m]
CPi1_Toluene_RT	45.17 ±0.63	43.00 ±0.52	2.17 ±0.11
CPW1_Toluene_RT	45.19 ±1.23	42.96 ±0.83	2.24 ±0.40
CPW3	44.85 ±0.48	43.32 ±0.42	1.53 ±0.06
CPW4_Toluene_RT	45.87 ±0.51	43.43 ±0.31	2.44 ±0.20
CPW5_Toluene_T50	44.56 ±1.17	43.23 ±0.81	1.33 ±0.35
CPW6	46.52 ±1.16	44.64 ±0.89	1.88 ±0.27
CTo1_Toluene_RT	44.18 ±1.45	42.14 ±1.14	2.05 ±0.32
CPi2_Heptane_RT	45.22 ±1.10	43.32 ±0.56	1.90 ±0.53
CTo2_Heptane_RT	44.73 ±0.50	43.22 ±0.27	1.51 ±0.23
SPW1_Heptane_RT	45.67 ±0.40	44.34 ±0.06	1.33 ±0.34
SPW4_Heptane_RT	46.50 ±1.28	45.56 ±0.97	0.94 ±0.31
IPW1_Heptane_RT	38.87 ±2.17	38.81 ±2.03	0.06 ±0.13
IPW4_Toluene_T50	40.52 ±1.44	40.49 ±1.37	0.03 ±0.08
BPA	66.79 ±0.24	27.29 ±0.04	39.50 ±0.20
BPi	63.79 ±0.16	31.19 ±0.05	32.60 ±0.11
BTo	62.13 ±0.60	28.68 ±0.34	33.45 ±0.25
BPW	57.21 ±0.70	28.96 ±0.21	28.24 ±0.49

Table 6: *Contact angle measurement results. Measurement names contain the sample ID followed by the last solvent used to anneal it (if any) and the temperature at which this annealing took place.*

6 Conclusion

Several experiments of annealing polymer films with solvent vapour of toluene and heptane have been executed, during which the film thicknesses have been monitored. When annealing with toluene vapour a thickness increase ranging from around 5% to 20% was observed, with the highest increase when analysing SI1 and SI7 with the oxide layer in the NanoCalc structure set to SiOx. When the oxide layer in the NanoCalc structure is set to SiO2_(therm) we generally observe an increase in thickness around 5%. This trend has been observed to occur with both homopolymer and diblock polymer films.

We saw that the homopolymer films from polystyrene swell 6.4% at room temperature and 4.9% at 50°C while polyisoprene swell 4.1% and 3.2%, so in this regard the increased temperature inside the chamber seems to lower the swelling behaviour. The two swelling curves for polystyrene do not show the same stepwise increase in thickness as the curves for polyisoprene. We ascribe this behaviour to decreased mobility in the styrene polymer chains caused by the high T_g of polystyrene. Since the T_g of polystyrene exceeds the temperature reached inside the chamber, we conclude based on [22] that the effective T_g of polystyrene must have been reduced enough to cause some motion. The behaviour is observed at both temperatures though less pronounced at $50°C$.

The poly(isoprene-*b*-styrene) diblock films CPi4 and CTo4, prepared on piranha cleaned and Topsil silicon wafers as received from the factory, both have approximately the same percent increase in thickness at around 5.4-5% when annealed with toluene at room temperature and at $50°C$. We do observe a slightly lower increase in thickness for the poly(isoprene-*b*-styrene) diblock film CPW4 cast on plasma cleaned Topsil wafers where the film swell 4.7%. We did not observe any notable difference in thickness when identical samples were annealed while maintaining a temperature of $50°C$ inside the vapour chamber; the diblock film CPi5 and CTo5 swells 5.3-4% while CPW5 4.8%. Though the temperature does not seem to have an influence on swelling behaviour, it is possible that the lower swelling of the films cast

on plasma cleaned wafers compared to the others, could be attributed to the cleaning method, but it is not entirely obvious in which way.

The thinnest diblock films ($<50nm$) do not really swell noticeably and we attribute this to the apparent influence low film thickness has on raising the T_g, therefore we end up with low mobility of the polymer chains in the film. In order to test this one would have to perform the experiment on a thicker film. We can conclude that heptane seems to be a poor choice for the solvent vapour when annealing the diblock thin films of $<50nm$ assuming our measurements are correct.

The surface free energy measurements for the diblock copolymer films are all in the range 44.18-46.52mN/m^2 and for the homopolymers we have 45.67mN/m^2 and 46.50mN/m^2 for polystyrene together with 38.87mN/m^2 and 40.52mN/m^2 for polyisoprene. Since the surface free energy for the diblock films is approximately equal to that of polystyrene, we conclude that polymers most likely are in a lammelae structure in the diblock film oriented horisontally with polystyrene in the top most layer. Furthermore, the diblock films were found to have a slightly higher polar part, with an average of 1.9mN/m, in comparison to the average of 1.14mN/m for polystyrene and 0.045mN/m for polyisoprene.

Finally we have learned about how many parameters that actually influence the solvent vapour annealing process, and how difficult it is to isolate the effects that each of these will have on the process. We have also learned that thin film thickness measurements using visible light spectroscopy during annealing has its limitations and ideally should not be used as the only source of information for swelling behaviour.

7 Perspective

Due to limited time and limited amount of sample size, we have not been able to confidently validate some of our findings. More data and analysing new data is needed. The following section is a combination of suggestions for further study and relevant observations not mentioned in the project itself.

In order to get more reliable results on the surface free energies, we would suggest to investigate the rather large difference between the measured and table values of the surface free energy of polyisoprene and polystyrene. It could be a result of our choice of images, that we did our contact angle measurements with, when determining the surface free energy. The first image chosen was taken about half a second after the drop hit the surface, allowing the surface to get dissolved by the liquids, thus disturbing the surface itself.

A suggestion on how to find out if this is the problem would be to measure contact angles frame for frame of the recorded video. Since the contact angle oscillates in the beginning, a reliable result can not be found at the first couple of frames. The longer the liquid is on the surface, the more polymer is getting absorbed by the liquid, thus compromising the surface itself, and therefore also the final result. The ideal image to do the contact angle measurement with, will therefore be when the drop stops oscillating - or some sort of average between the contact angle at the images prior to.

If these images do not give better results, the deviation might be caused by the liquids having dissolved to much polymer at the time a reliable measurement can be executed, or that the surface exhibits roughness. The roughness of the surface affect the contact angle[23], and therefore also the measurement of the surface free energy.

Shortly prior to handing in the project, we observed, while looking at the videos from the contact angle device, that wetting happens much faster on the BPA1 wafer and much slower on BPi1 compared to the other blank wafers. We have normalised the diameter of the drops at around the 4 to 36

seconds mark after the drop has been placed, and found the following relative increments (table 7). If we had more blank wafers, we would have replicated

	BPA	BPi	BPW	BTo
Relative increase in diameter - Water	10.23%	0.33%	4.95%	2.97%
Relative increase in diameter - Diiodomethane	6.51%	2.68%	3.45%	4.60%
Surface free energy $[mN/m]$	66.79	63.79	57.21	62.13

Table 7: *Relative increase in drop diameter during contact angle measurements on blank wafers.*

the experiments. We would suggest doing the contact angle measurements straight after cleaning, instead of waiting several months. If results like these show again, then there is strong evidence that the cleaning methods affect the wafers.

Preliminary results from our supervisor Dorthe suggest that Piranha cleaning changes the structure of the wafer surface, which might be the cause of the almost non existing wetabillity on BPi1. According to [13] plasma cleaning with air can cause oxidisation, encourage hydroxylation, thus making the surface more hydrophilic, thus explaining faster wetting of blank plasma cleaned wafers.

If this indeed is the case, using the same reference file in NanoCalc for all the wafers might have affected the final results when doing optical spectroscopy, especially if the plasma cleaning has caused oxidisation. Even though undocumented, we have recently observed that references made at different temperatures give different results when measuring thicknesses. Therefore an investigation of the importance of the reference file is suggested. The ideal reference would be made straight after cleaning, since R_{ref} in NanoCalcs version (see equation 4.1) does not take the oxide layer into account [16], even if native oxide is present when measuring I_{ref}. After having reread the NanoCalc manual it was noticed that it suggests that the reference measurement has to be repeated from time to time, due to drift of lamps and so on, especially when measuring film layers with thin thicknesses as has been

the case in this project. The manual does not mention how often to redo the reference. As dark inside the chamber we suggest using Vantablack from Surrey Nanosystems, since this material supposedly has one of the lowest reflectance in the world.

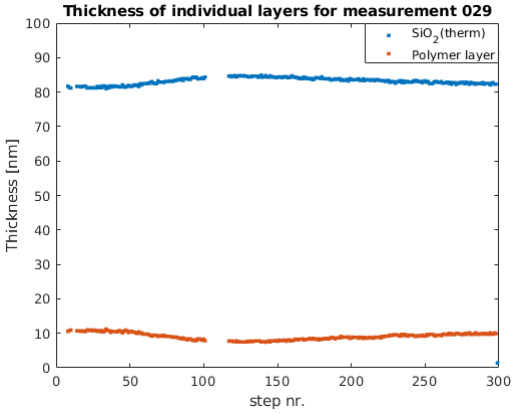

Figure 7.1: *Thickness of non-existing oxide and polymer layer plotted again the number of timesteps, while heating and cooling the wafer in the chamber. Measurements have been omitted since they were made using the layer SiOx*

As seen in the logbook, temperature effects on the polymers and measurements itself have been considered greatly. These have not been included since we have not been able to explain these data, until recently when we discovered that T_m for polyisoprene is about 35.5°C. Even though undocumented, prior to the first swelling for IS1 at 50°C, we noticed that the thickness decreased while the temperature of the chamber increased.

Due to an unknown mistake when making a reference and dark (ID 005 in the logbook) for thickness measurement of the homopolymer layers, NanoCalc proposed a $\sim 80nm$ SiO2_(therm) layer and $\sim 10nm$ polymer layer (measurement 028 in the logbook) on this same blank reference wafer at room temperature. In heat measurement 029 we increased the temperature from 26.2°C to 50°C and then back to 26.7°C. The thickness of the oxide and non-existing polymer layer is plotted in figure 7.1

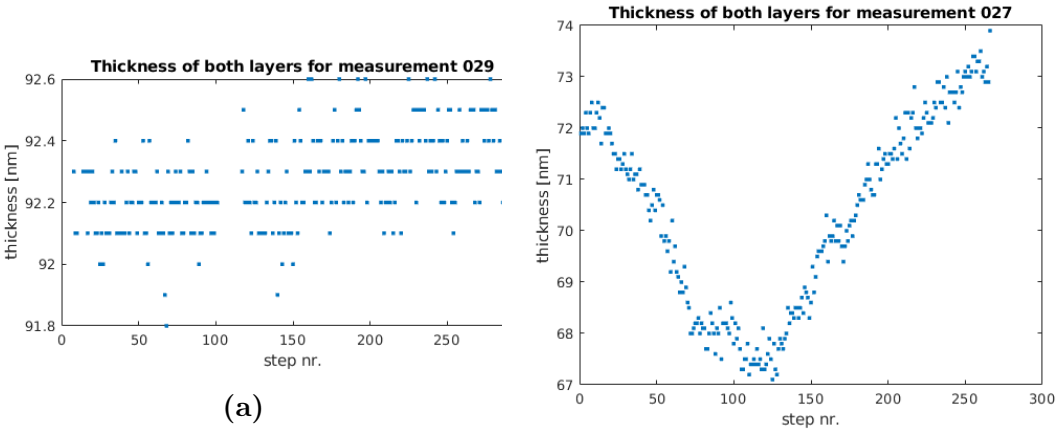

Figure 7.2: ***a)*** *Combined thickness of non-existing oxide and polymer layer plotted against the number of timesteps, while heating and cooling the wafer in the chamber. Note there is only a 0.8nm difference* ***b)*** *Combined thickness of SiO2_(therm) and block copolymer layer on IS6 plotted against the number of timesteps, while heating and cooling the wafer in the chamber*

Since the temperature is not logged automatically with the measurements, we can not plot the thickness-temperature dependence. Since this wafer is blank, decrease in polymer thickness proposes that the reflected light of the spectrometer might be affected by the temperature of the contents of the chamber. But if we sum the SiO2_(therm) and polymer thickness from heat measurement 029, we see an relatively constant thickness (figure 7.2a). Almost constant thickness is what one would expect when measuring a non-existing polymer layer, which is why we assume that the sum is more accurate for this measurement. In measurement 027 we did the same heat dependent experiment for our university block copolymer wafer IS6. The sum of the SiO2_(therm) and polymer thickness of measurement 027 is plotted in 7.2b. It is clearly seen that the thickness is not constant for measurement 027.
While the temperature increased from 28 to 45.1°C in measurement 027, we added the temperature to the comments in the data. The temperature-film thickness dependence is plotted in figure 7.3. Here it is quite clear, that the thickness begins to drop around the 39°C mark, which is only 4.5°C above the melting point of polyisoprene. Further study into temperature behaviour

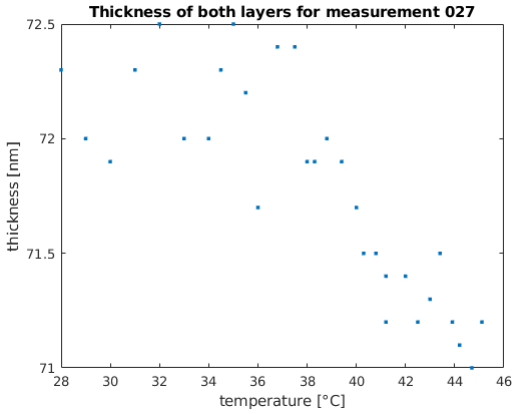

Figure 7.3: *Temperature-thickness dependence plotted from measurement 027.*

is recommended.

We have also noticed that NanoCalc uses a refractive index for each wavelength, resulting in that using the constants "n1_5", "n1_55" and "n1_6" is not entirely accurate for the polymers. At the same time, we also noticed that it is possible to customise your own .dat file with n values, such that polyisoprene and polystyrene can be added. NanoCalc is then able to do mixtures of different layers, meaning that it is possible to combine the polyisoprene and polystyrene into one layer. It is also possible to take the refractive index of the swollen polymers into consideration using this method, since the refractive indices of the solvent can be mixed with the ones for the polymers.

References

[1] P. Müller-Buschbaum, "Influence of surface cleaning on dewetting of thin polystyrene films," *The European Physical Journal E*, vol. 12, no. 3, pp. 443–448, 2003.

[2] J. E. Mark, *Physical properties of polymers handbook*. Springer, 2. ed. ed., 2007.

[3] V. Arrighi and J. Cowie, *Polymers: Chemistry and Physics of Modern Materials, Third Edition*. CRC Press, 3rd ed ed., 2007.

[4] M. J. Fasolka and A. M. Mayes, "Block copolymer thin films: Physics and applications," *Annual Review of Materials Research*, vol. 31, pp. 323–55, 2001.

[5] "Ossila spin coating: A guide to theory and techniques." `https://www.ossila.com/pages/spin-coating`. Accessed: 2018-12-30.

[6] J. H. Kim, J. Jang, and W.-C. Zin, "Thickness dependence of the glass transition temperature in thin polymer films," *Langmuir*, vol. 17, no. 9, pp. 2703–2710, 2001.

[7] T. Tadros, "Flory-huggins interaction parameter," in *Encyclopedia of Colloid and Interface Science* (T. Tadros, ed.), pp. 523–524, Berlin, Heidelberg: Springer Berlin Heidelberg, 2013.

[8] C. Sinturel, M. Vayer, M. Morris, and M. A. Hillmyer, "Solvent vapor annealing of block polymer thin films," *Macromolecules*, vol. 46, no. 14, pp. 5399–5415, 2013.

[9] D. Harrison, W. Ellis, and H. C. Ohanian, *Physics for engineers and scientists*. W.W. Norton, 2008.

[10] A. W. Adamson and A. P. Gast, *Physical Chemistry of Surfaces*. A Wiley-Interscience publication, Wiley, 6. ed. ed., 1997.

[11] DataPhysics Instruments GmbH, *Interfacial Chemistry - Introduction into Methods of Measuring and Analyzing Contact Angles for the Determination of Surface Free Energies of Solids.* http://www.kt.dtu.dk/-/media/Centre/DPC/dpc/english/Instrumentation/CAG/CAG-manual.ashx Accessed: 2019-1-2.

[12] "Plasma Etch what is plasma treatment?." http://www.plasmaetch.com/plasma-treatment-basics.php. Accessed: 2018-11-30.

[13] "Harrick Plasma: Plasma cleaning." http://harrickplasma.com/applications/plasma-cleaning. Accessed: 2018-11-30.

[14] Princeton University Office of Environmental Health and Safety, https://ehs.princeton.edu/laboratory-research/chemical-safety/chemical-specific-protocols/piranha-solutions, *Piranha Solutions.* Laboratory Safety Manual.

[15] W. Bohling, Christian;Sigmund, "Self-limitation of native oxides explained," *Springer Science+Business Media*, dec 2015.

[16] Ocean Optics Inc., *NanoCalc Software 4.0 software manual - Analysis Software for Thin Film Metrology.*

[17] G. Ström, M. Fredriksson, and P. Stenius, "Contact angles, work of adhesion, and interfacial tensions at a dissolving hydrocarbon surface," *Journal of Colloid And Interface Science*, vol. 119, no. 2, pp. 352–361, 1987.

[18] CR, "Predicting the dispersability of particles," application report, KRÜSS, jan 2000.

[19] Z. Di, D. Posselt, D.-M. Smilgies, R. Li, M. Rauscher, I. Potemkin, and C. Papadakis, "Stepwise swelling of a thin film of lamellae-forming poly(styrene-b-butadiene) in cyclohexane vapor," *Macromolecules*, vol. 45, no. 12, pp. 5185–5195, 2012.

[20] M. N. Polyanskiy, "Refractive index database." https://refractiveindex.info. Accessed: 2019-01-02.

[21] "JitBit macro recorder." `https://www.jitbit.com/macro-recorder`. Accessed: 2018-12-30.

[22] A. Yoshioka and K. Tashiro, "Solvent effect on the glass transition temperature of syndiotactic polystyrene viewed from time-resolved measurements of infrared spectra at the various temperatures and its simulation by molecular dynamics calculation," *Macromolecules*, vol. 37, no. 2, pp. 467–472, 2004.

[23] R. Wenzel, "Surface roughness and contact angle," *Journal of Physical Colloid Chemistry*, vol. 53, no. 9, pp. 1466–1467, 1949.

A Appendix

A.1 Contact Angles - Water

Measurement name	water (Air) Mean CA(l) [°]	water (Air) Mean CA(r) [°]	water (Air) Mean CA(m) [°]
CPi1_Toluene_RT	82.26 (±0.30)	82.75 (±0.36)	82.50 (±0.33)
CPW1_Toluene_RT	82.20 (±1.46)	82.38 (±1.39)	82.29 (±1.43)
CPW3	85.01 (±0.13)	85.04 (±0.12)	85.03 (±0.10)
CPW4_Toluene_RT	81.31 (±0.70)	81.24 (±0.69)	81.27 (±0.69)
CPW5_Toluene_T50	85.98 (±1.72)	86.04 (±1.63)	86.01 (±1.67)
CPW6	82.60 (±0.98)	82.91 (±0.98)	82.75 (±0.98)
CTo1_Toluene_RT	83.48 (±1.07)	83.49 (±1.07)	83.49 (±1.07)
CPi2_Heptane_RT	83.41 (±2.16)	83.44 (±2.15)	83.42 (±2.16)
CTo2_Heptane_RT	84.92 (±1.05)	85.39 (±1.09)	85.15 (±1.07)
SPW1_Heptane_RT	85.26 (±1.66)	85.53 (±1.65)	85.39 (±1.65)
SPW4_Heptane_RT	86.74 (±1.74)	86.88 (±1.76)	86.81 (±1.75)
IPW1_Heptane_RT	98.52 (±2.83)	99.10 (±2.95)	98.81 (±2.88)
IPW4_Toluene_T50	98.70 (±2.36)	98.48 (±2.26)	98.59 (±2.31)
BPA	25.22 (±0.42)	25.62 (±0.41)	25.42 (±0.42)
BPi	32.66 (±0.11)	33.79 (±0.25)	33.22 (±0.18)
BTo	35.40 (±0.13)	34.10 (±0.14)	34.75 (±0.13)
BPW	42.72 (±0.70)	43.01 (±0.76)	42.86 (±0.73)

Table 8: *Contact angles measured with water. Measurement names contain the sample ID followed by the last solvent used to anneal it (if any) and the temperature at which this annealing took place.*

A.2 Contact Angles - Diiodomethane

Measurement name	diiodo-methane (Air) Mean CA(l) [°]	diiodo-methane (Air) Mean CA(r) [°]	diiodo-methane (Air) Mean CA(m) [°]
CPi1_Toluene_RT	31.97 (±0.41)	33.74 (±1.96)	32.85 (±1.16)
CPW1_Toluene_RT	33.60 (±2.04)	32.31 (±1.70)	32.95 (±1.87)
CPW3	32.42 (±1.17)	31.81 (±0.82)	32.11 (±0.97)
CPW4_Toluene_RT	32.03 (±1.54)	31.71 (±0.56)	31.87 (±0.72)
CPW5_Toluene_T50	32.84 (±2.15)	31.83 (±1.71)	32.33 (±1.85)
CPW6	31.59 (±3.24)	26.36 (±2.04)	28.97 (±2.22)
CTo1_Toluene_RT	35.20 (±2.59)	34.33 (±2.85)	34.77 (±2.47)
CPi2_Heptane_RT	31.74 (±1.31)	32.51 (±1.29)	32.12 (±1.30)
CTo2_Heptane_RT	32.17 (±0.57)	32.54 (±0.66)	32.35 (±0.61)
SPW1_Heptane_RT	29.56 (±0.11)	29.85 (±0.37)	29.70 (±0.15)
SPW4_Heptane_RT	25.03 (±1.26)	28.20 (±4.05)	26.61 (±2.57)
IPW1_Heptane_RT	41.17 (±4.04)	41.96 (±3.87)	41.56 (±3.96)
IPW4_Toluene_T50	38.47 (±2.81)	37.99 (±2.78)	38.23 (±2.79)
BPA	62.56 (±0.28)	61.89 (±0.17)	62.22 (±0.06)
BPi	55.10 (±0.08)	55.79 (±0.10)	55.45 (±0.09)
BTo	59.35 (±0.53)	60.27 (±0.66)	59.81 (±0.60)
BPW	59.03 (±0.38)	59.62 (±0.34)	59.33 (±0.36)

Table 9: *Contact angles measured with Diiodomethane. Measurement names contain the sample ID followed by the last solvent used to anneal it (if any) and the temperature at which this annealing took place.*

A.3 Thickness Measurements of Oxide layer

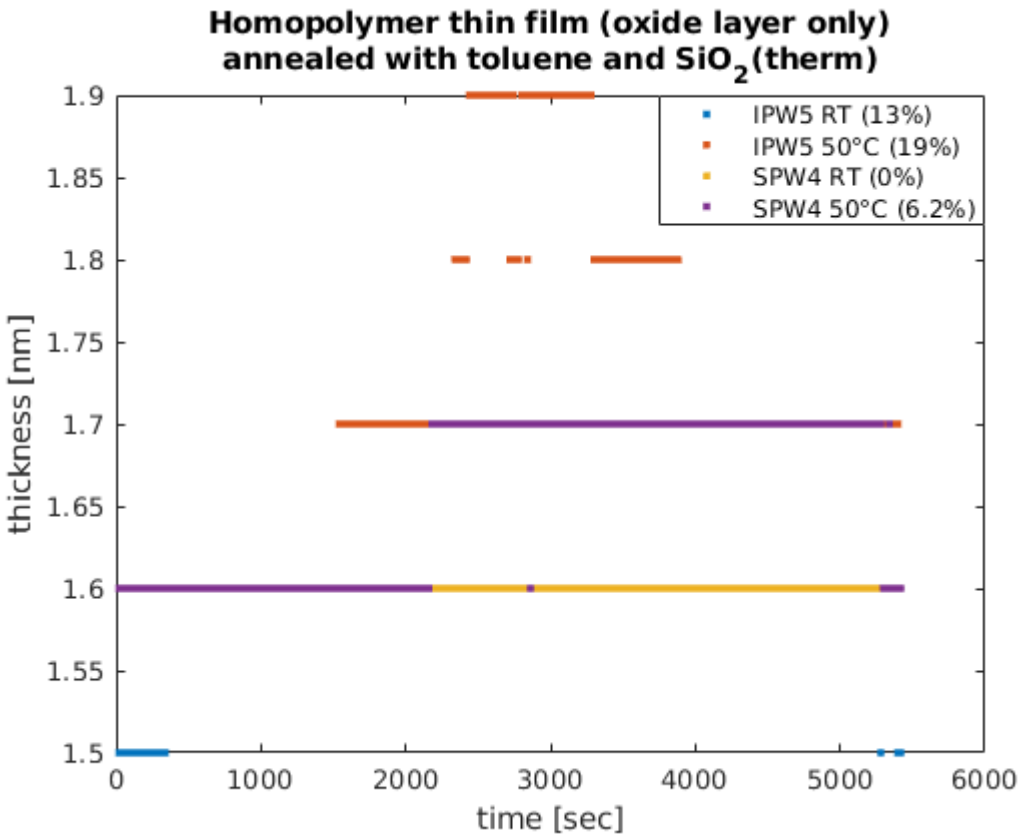

Figure A.1: *Thickness of the oxide layer for the polyisoprene and polystyrene annealed at room temperature and at 50°. The oxide layer has been set to SiO_2(therm). It is clear from the graph that the oxide layer thickness measurements overlap.*

A.4 Logbook explanation

The list explaining each of the column entries in the excel spreadsheet follows below:

Date and ID: Specifies the date and ID number of the entry

Type: Specifies the type of entry in the logbook. RefDark is the creation of a file with the dark and reference. Measure is pure thickness measurement. Swelling is measurement of thickness during swelling. Heat is experiments where thickness behaviour is observed during changing temperatures.

Wafer: Which wafer was used. The parenthesis is referring to the number in Sina's table.

RefDark: Mentions which refDark was used during this entry. The number in parenthesis refers to the ID number of the refDark

Dark: The dark used during the creation of the refDark file.

Integration time: The integration time using during the creation of the refDark file

Purpose: The purpose of the entry

Oxide layer: The type of oxide layer used for measurements

Ox est: The estimation of the oxide layer thickness

Film layer est: The estimation of the film layer thickness

Refr index: The refractive index used for the polymer

Thic ox_start: The thickness of the oxide layer before adding vapour to the chamber

Thic po_start: The thickness of the polymer layer before adding vapour to the chamber

Temp: The temperature of the chamber during experiment. "a-b-c" refers to a entry of type Heat where a is the start temperature, b is the max temperature, end c is the end temperature.

Thic_ox_atMaxPo: The thickness of the oxide layer when the polymer achieves its biggest value during swelling.

Thic_po_Max: The maximum thickness of the polymer during swelling

Rel swell: The relative swelling during the entry

Fit: The fitness of the experiment. Bad is more than 1.... continue

Comment: Comments needed to be added to this entry. This can be done several days after the entry has been added to the logbook.

RefDark filename: The name of the refDark file used

Data filename: The name of the textdocument containing the logfile data from the entry. maybe explain further